Received: 30 September 2021 | Revised: 20 April 2023 | Accepted: 13 May 2023

DOI: 10.1111/geb.13705

Global Ecology and Biogeography A Journal of Macroecology

WILEY

RESEARCH ARTICLE

Global depth distribution of belowground net primary productivity and its drivers

Liujun Xiao[1,2] | **Guocheng Wang**[3] | **Jinfeng Chang**[1,4,5] | **Yaoyao Chen**[1] | **Xiaowei Guo**[1] | **Xiali Mao**[1] | **Mingming Wang**[1] | **Shuai Zhang**[1] | **Zhou Shi**[1,4,5] | **Yiqi Luo**[6] | **Lei Cheng**[7] | **Kailiang Yu**[8] | **Fei Mo**[9] | **Zhongkui Luo**[1,4,5]

[1]College of Environmental and Resource Sciences, Zhejiang University, Hangzhou, China

[2]National Engineering and Technology Center for Information Agriculture, Engineering Research Center of Smart Agriculture, Ministry of Education, Key Laboratory for Crop System Analysis and Decision Making, Ministry of Agriculture, Jiangsu Key Laboratory for Information Agriculture, Jiangsu Collaborative Innovation Center for Modern Crop Production, Nanjing Agricultural University, Nanjing, China

[3]Faculty of Geographical Science, Beijing Normal University, Beijing, China

[4]Academy of Ecological Civilization, Zhejiang University, Hangzhou, China

[5]Key Laboratory of Environment Remediation and Ecological Health, Ministry of Education, Zhejiang University, Hangzhou, China

[6]Center for Ecosystem Science and Society, Department of Biological Sciences, Northern Arizona University, Flagstaff, Arizona, USA

[7]Department of Hydrology and Water Resources, School of Water Resources and Hydropower Engineering, Wuhan University, Wuhan, China

[8]High Meadows Environmental Institute, Princeton University, Princeton, New Jersey, USA

[9]College of Agronomy, Northwest A&F University, Xianyang, China

Correspondence

Zhongkui Luo, College of Environmental and Resource Sciences, Zhejiang University, Hangzhou, Zhejiang, China.
Email: luozk@zju.edu.cn

Funding information

Foundation for Fundamental Research of China, Grant/Award Number: 2021YFE0114500; National Natural Science Foundation of China, Grant/Award Number: 42001105, 32171639 and 32241036; State Key Laboratory of Atmospheric Boundary Layer Physics and Atmospheric Chemistry, Grant/Award Number: LAPC-KF-2022-10

Handling Editor: Franziska Schrodt

Abstract

Aim: This study aimed to infer the allocation of belowground net primary productivity (BNPP) to sequential soil depths down to 2 m across the globe at a 1 km resolution and assess underlying environmental drivers.

Location: Global.

Time Period: Contemporary (1932–2017).

Major Taxa Studied: Terrestrial plants.

Methods: Global datasets including field net primary production (NPP, i.e., the difference between plant assimilated and respired carbon) from 725 soil profiles, root biomass and its depth distribution from 559 soil profiles were compiled and used to infer the depth distribution of BNPP across the globe and digitally map depth-resolved BNPP globally at 1 km resolution. Drivers of the depth distribution of BNPP were evaluated using machine learning-based models.

Results: Global average BNPP allocated to the 0–20 cm soil layer is estimated to be 1.1 Mg C $ha^{-1}yr^{-1}$, accounting for ~60% of total BNPP. Across the globe, the depth distribution of BNPP varies largely, and more BNPP is allocated to deeper layers in hotter and drier regions. Edaphic, climatic and topographic properties (in order of importance) explain >80% of such variability; and the direction and magnitude of the influence of individual properties are soil depth- and biome-dependent.

Main Conclusions: The findings suggest that mean annual temperature and precipitation are the two most important factors regulating BNPP across the globe. Soil properties such as soil actual evaporation and total nitrogen also play a vital role in regulating the depth distribution of BNPP. The maps of BNPP provide global benchmarks of depth-resolved BNPP for the prediction of whole-profile soil carbon dynamics across biomes.

KEYWORDS
carbon inputs, global mapping, net primary productivity, root biomass, root profile, vertical distribution

1 | INTRODUCTION

Plant net primary productivity (NPP), which is defined as the difference between plant gross primary productivity and autotrophic respiration, is a fundamental ecosystem property, providing food, energy and fibre for higher trophic organisms and mediating the globe carbon cycle by linking atmospheric and soil carbon reservoirs (Green et al., 2019; Imhoff et al., 2004; Krausmann et al., 2013). In mineral soils—the largest terrestrial carbon reservoir (Batjes, 2016), belowground NPP (BNPP) represents the key carbon input to soil, together with soil carbon outputs mainly via microbial decomposition, determining soil carbon balance. Along soil profile, the depth distribution of BNPP is critical for understanding whole-soil profile carbon dynamics and plant–soil interactions. First, the vertical distribution of BNPP couples with a series of belowground processes such as plant water uptake and nutrient acquisition which are important processes modulating plant growth (e.g., rooting depth) and its response to environmental changes (Greiner et al., 2017). Second, new carbon inputs represented by BNPP to different soil depths influence soil carbon turnover behaviours in different layer depths (Luo et al., 2019) by providing energy-rich substrates to soil microbes. For example, the new carbon may actively, but distinctly, interact with existing soil carbon in different soil depths via the priming effect (i.e., new carbon promotes or retards native carbon decomposition) (Cheng et al., 2014; Kuzyakov, 2010), regulating whole-soil carbon stability (Luo et al., 2020). It is vital to quantify the depth distribution of BNPP to elucidate belowground processes and making reliable depth-specific predictions of plant–soil interactions, soil carbon and relevant biogeochemical cycles (e.g., nutrients and greenhouse gas emissions) in the soil profile.

A number of approaches have been developed to measure BNPP in different ecosystems using root growth measurements (e.g., ingrowth cores) (Davidson et al., 2002; Garnier, 1991; Raich & Nadelhoffer, 1989) or state-of-the-art tracer (e.g., carbon isotopes) techniques (Balesdent et al., 2018). Although potential uncertainties in BNPP estimates using different approaches, data synthesis based on total BNPP measurements with uncertainty assessment would help us address critical questions relating to soil carbon dynamics such as carbon turnover times based on the ratio of soil carbon stocks to BNPP at large spatial scales (Fan et al., 2020; Luo et al., 2019). BNPP has also been indirectly estimated. For example, by synthesizing field measurements of aboveground NPP (ANPP), combining with satellite-derived NPP, total BNPP has been quantified as the difference between satellite-derived NPP and ANPP (Gherardi & Sala, 2020). However, large-scale in situ application of these approaches for depth-specific quantification of BNPP is challenging due to technology and cost limitations (Le Quéré et al., 2018; Malhi et al., 2017). Indeed, few studies have un-destructively and directly measured BNPP depth by depth in situ (Malhi et al., 2017). Existing experimental and modelling studies requiring depth-specific BNPP as inputs usually used root biomass profiles to infer the depth allocation of BNPP by adopting certain assumptions on the relationship between vertical distribution of root biomass and BNPP (Camino-Serrano et al., 2018; Luo et al., 2019; Xu et al., 2014). Without depth-resolved quantification of BNPP, our confidence of sustainable land management (e.g., identifying management practices for soil carbon sequestration) and whole-soil biogeochemical process understanding (e.g., soil carbon balance and greenhouse gas emissions) would be undermined.

Moreover, factors controlling BNPP and particularly their depth distribution may be diverse and vary across space (McCormack et al., 2015; Zhang & Wang, 2015). In Earth system models, which are major tools predicting global carbon cycle, however, BNPP and its depth distribution are usually assumed to be a constant fraction of total carbon assimilated by plants depending on plant functional types and climate is generally considered to be the dominant determinant (Friedlingstein et al., 2006; Zhao & Running, 2010). This simplification of controls over depth distribution of BNPP would be the major source of the uncertainty in predictions of soil carbon-climate feedbacks as well as belowground processes such as soil carbon sequestration potential across space and over time (Cramer et al., 2001). Across global grasslands, for example, observational data synthesis focusing on total NPP and its aboveground and belowground fractions found that mean annual temperature is the most important factor influencing BNPP (Sun et al., 2021), but they also emphasized that non-climatic variables such as soil and topography might be also important but are less explored. Another global scale study indicated that BNPP increases with mean annual precipitation (MAP), but the increase rate decreases with MAP (Gherardi & Sala, 2020). In addition, they found that different biomes show distinct relationships between BNPP and MAP, and MAP can only explain 36% of the variance of BNPP across the globe. However, controls over the depth allocation of BNPP are rarely assessed and remain uncertain. Overall, we need an advanced understanding of whether and how soil depth-specific carbon inputs vary among vegetation types and are modulated by other environmental factors such as edaphic and topographic attributes.

Building upon global datasets of field measurements of plant assimilated carbon (i.e., NPP) with its partitioning of aboveground and belowground fractions (i.e., ANPP and BNPP) and the vertical distribution of root biomass, this study aims to: (1) estimate the allocation of BNPP to seven sequential soil layers (i.e., 0–20, 20–40, 40–60, 60–80, 80–100, 100–150 and 150–200 cm); (2) assess underlying drivers regulating the depth distribution of BNPP across the globe and biome types; (3) map the depth distribution of BNPP and its uncertainty across the globe at the resolution of 0.0083° (which is equivalent to ~1 km at the equator). This information is essential to improve future accounting of whole-soil carbon balance and relevant greenhouse gas emissions across large scales.

2 | MATERIALS AND METHODS

A flowchart (Figure S1) was produced to show the method and procedure used for the estimation of the depth distribution of BNPP and its drivers. Detailed steps are described in the following Sections 2.1–2.7.

2.1 | Net primary productivity (NPP)

We collected a global dataset of field measurements of NPP including 725 soil profiles across the globe (Figure 1a; NPP_{obs} hereafter). NPP_{obs} contains NPP, the fraction of NPP allocated belowground (BNPP), and/or aboveground NPP (ANPP), enabling us to directly calculate BNPP. The dataset was compiled by a thorough literature search and data synthesis from 54 published peer-reviewed papers (literature-derived dataset, Appendix A—Data Sources) and the ORNL DAAC NPP data collection (https://daac.ornl.gov/cgi-bin/dataset_lister.pl?p=13). Although field methods for estimating BNPP vary somewhat from site to site, it is common that BNPP in woody vegetation was estimated based on the amount and turnover of live and dead fine root biomass (which were measured in periodically sampled soil or ingrowth cores) and coarse root biomass (which was measured by excavated trenches). In grasslands, BNPP was generally estimated by extracting belowground biomass samples from soil or ingrowth cores to calculate total net root production. Here we note that soil and ingrowth cores are the two dominant approaches used for field BNPP measurements in the literature-derived dataset (48 of the 54 papers, Table S1). By grouping BNPP into soil and ingrowth core measurements, the results suggested that BNPP across the globe as well as for the same biome is comparable between the measurement approaches (Figure S2). So, in this study, we did not explicitly distinguish different measurement approaches in the following data assessment.

It should be noted that the ORNL DAAC dataset is quality-controlled (e.g., mapping the points in geographical space to confirm that they coincided with landforms, and checking data ranges for outliers and errors) in order to minimize the potential effects of different measurement techniques on the estimation of NPP and its allocation. However, the detailed quality-control procedure cannot be retrieved and applied to the literature-derived dataset. Rather, we conducted a comparison between the literature-derived dataset and the ORNL DAAC dataset (Figure S3). The two datasets predicted similar ($p > 0.05$) BNPP in most ecosystems except in forests and shrublands (Figure S3a,b). In addition, the two datasets presented a very similar latitudinal pattern of BNPP and were complementary in terms of both spatial (Figure S3a) and latitudinal coverage (Figure S3c). For these reasons, we pooled data together to increase spatial coverage.

2.2 | Root biomass

We obtained root biomass and its depth distribution from 559 soil profiles to infer the depth distribution of BNPP (see Section 2.5). This root biomass dataset ($Root_{obs}$ hereafter) was originally compiled by Schenk and Jackson (2002). In this study, we assumed that the vertical distribution of BNPP is comparable to that of root biomass because root productivity is the predominant contributor to BNPP (Gherardi & Sala, 2020; Yuan & Chen, 2010), an approach used in other studies (Luo et al., 2019; Xu et al., 2014).

2.3 | Environmental covariates

A set of global layers of environmental covariates including soil properties, climate and topography (Table S2) were collected as potential predictor variables of BNPP and its depth distribution. A total of 20 soil physical and chemical properties (Table S3) were obtained from ISRIC-WISE soil profile database (Batjes, 2016) with a spatial resolution of 1 km. Nineteen climatic attributes with the same resolution as the WISE database were obtained from WorldClim (Fick & Hijmans, 2017) which quantifies biologically meaningful climatic variables using monthly temperature and precipitation. Actual soil evaporation (AE) calculated as liquid water supply plus soil water utilized was obtained from TerraClimate (Abatzoglou et al., 2018). We also calculated 13 topographic attributes (Table S3) from SRTM-DEM at 90 m resolution (http://srtm.csi.cgiar.org) using “elevatr”, “spatialEco” and “dynatopmodel” packages in R 4.1.2 (R Development Core Team, 2021) and a widely used module SAGA GIS with popular terrain analysis tools (Conrad et al., 2015). More details of estimating global topographic attributes can be found in Amatulli et al. (2018).

2.4 | Biomes

We derived biome types from a biome classification map of the Terrestrial Ecoregions of the World (Olson et al., 2001) that is widely used in contemporary biogeographical research. This map considers

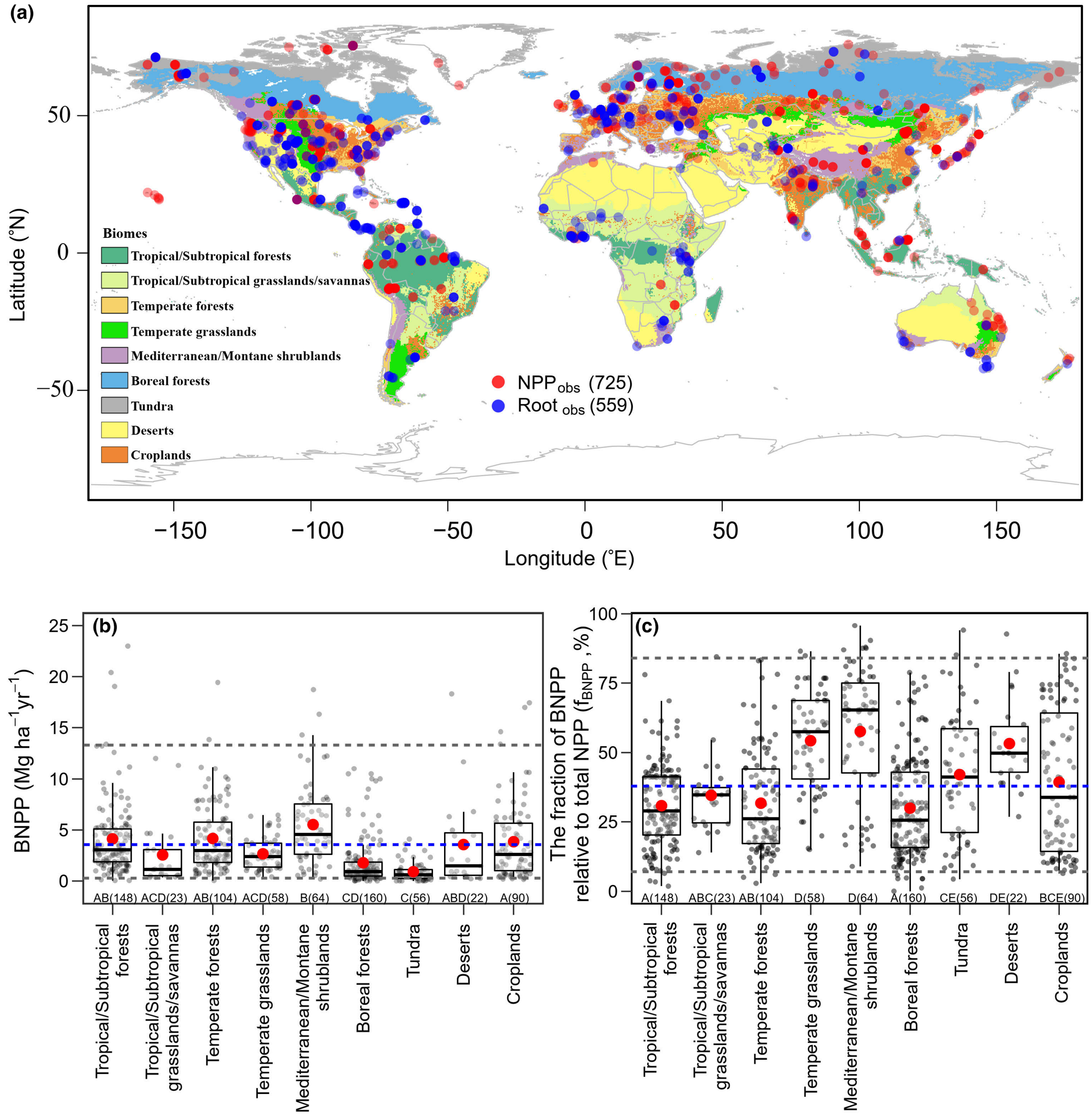

FIGURE 1 Net primary productivity (NPP) and their depth distribution. (a) The location of soil profiles with in situ measurements of NPP with its above- and belowground fractions (NPP$_{obs}$) and the depth distribution of root biomass (Root$_{obs}$). (b) The distribution of BNPP among nine biomes. (c) The fraction of BNPP (f_{BNPP}) relative to total NPP inferred from NPP$_{obs}$. Boxplots show the median and interquartile range with whiskers extending to 1.5 times of the interquartile range, and red dots show averages. Different capital letters below the boxes indicate significant differences ($p < 0.05$) among biomes, and numbers in parentheses show sample size. Blue dashed lines show the average, and the upper and lower grey dashed lines show the 97.5% 2.5% quantiles.

species distribution, ecoregions and biogeographical realms as basic criteria for biome class assignment, generally aligning with the fact that BNPP is an ecosystem property influenced by a series of ecological processes and patterns. To take into account the effect of human land use (i.e., croplands), MODIS land cover map (Channan et al., 2014) was overlapped with the biome map. Finally, a map consisting of nine biome types was obtained: tropical/subtropical forests, tropical/subtropical grasslands/savannas, temperate forests, temperate grasslands, Mediterranean/montane shrublands, boreal forests, tundra, deserts and croplands (Figure 1a).

2.5 | Estimation of the depth distribution of BNPP

Total BNPP has been recorded in the NPP_{obs} dataset. We assumed that BNPP allocated to a specific layer depth is proportional to root biomass in that layer. Using the Root_{obs} dataset, we calculated the depth distribution of root biomass in seven sequential layers in the 0–200 cm soil profile (i.e., 0–20, 20–40, 40–60, 60–80, 80–100, 100–150 and 150–200 cm), using the following equations (Jochen & Jackson, 2002; Luo et al., 2019):

$$r_D = \frac{R_{\max}}{1 + \left(\frac{D}{D_{50}}\right)^c}, \tag{1}$$

where r_D is the total root biomass above soil depth D (cm), $R_{\max}$ is the total root biomass of the whole soil profile, D_{50} is the depth (cm) at which r_D is 50% of $R_{\max}$ and c is the shape parameter optimized by the Root_{obs} dataset (Jochen & Jackson, 2002):

$$c = \frac{-1.27875}{\log_{10} D_{95} - \log_{10} D_{50}}, \tag{2}$$

where D_{95} is the depth (cm) at which r_D is 95% of $R_{\max}$. According to Equation (1), the fraction (f_{root}) of roots in any soil layer depths such as the 20–40 cm soil layer depth can be estimated as:

$$f_{\text{root},20-40} = \frac{r_{40}}{r_{\max}} - \frac{r_{20}}{r_{\max}} = \frac{1}{1 + \left(\frac{40}{D_{50}}\right)^c} - \frac{1}{1 + \left(\frac{20}{D_{50}}\right)^c} \tag{3}$$

The Root_{obs} had been used to interpolate D_{50} and D_{95} (Jochen & Jackson, 2002; Luo et al., 2019), which have been adopted here. Based on the Root_{obs}-derived proportional depth distribution of roots, we trained a machine learning-based model (Figure S4) to predict the proportional depth distribution of BNPP at NPP_{obs} sites. Then, BNPP in a typical layer such as 20–40 cm can be estimated as BNPP multiplied by the proportion of BNPP in that layer (Figures 2 and S5). Tukey's HSD test was used to determine if BNPP in different soil depths and among biomes are significantly different.

We acknowledge that an assumption of the vertical distribution of BNPP being equal to the vertical distribution of root biomass is adopted in this study to facilitate global scale quantification. To test this assumption, we used a depth-resolved two-pool root turnover model—ORCHIDEE-SOM (Camino-Serrano et al., 2018) to infer the depth distribution of BNPP. In the model (Camino-Serrano et al., 2018), roots have been divided into metabolic and structural roots with fast and slow turnover rates respectively. In each layer *z*, root turnover for each pool *i* (i.e., metabolic and structural) is described by first-order kinetics:

$$\frac{\partial RootC_{i,z}}{\partial t} = I(t)_{i,z} - kRootC_i \times RootC_{i,z}(t) \times \theta(t) \times \tau(t) \tag{4}$$

where $I(t)_{i,z}$ is the carbon input to the *i*th root pool at soil depth of *z* at time *t*, *kRootC* is the root turnover rate constant with a default value of 0.5 yr^{-1} for metabolic roots and 3.0 yr^{-1} for structural roots. In the model, the fraction of metabolic roots is equal to 0.85–0.018 × LC (root lignin:carbon ratio) × CN (root carbon:nitrogen ratio), and the remaining fraction is structural roots, and the default values of LC (0.22) and CN (40) in the model were used. θ and τ are two rate modifiers of soil moisture and temperature respectively. Soil moisture and temperature (BIO1) data used can be found in Table S3. Quantitatively, $I(t)_{i,z}$ in the model is equal to BNPP (i.e., root-derived carbon inputs) in that layer, that is, $I(t)_{i,z} = \text{BNPP}(t)_{i,z}$. At steady state, $\text{BNPP}(t)_{i,z}$ can be estimated as:

$$\text{BNPP}(t)_{i,z} = I(t)_{i,z} = kRootC_i \times RootC_{i,z}(t) \times \theta(t) \times \tau(t) \tag{5}$$

We run the model at a time step of 1 year at Root_{obs} sites ($N = 559$) using observed *RootC* (i.e., root biomass) to estimate BNPP. Then, the proportional allocations of *I*(*t*) (i.e., BNPP) and *RootC* to each soil layer were used to test whether the vertical distributions of BNPP and root biomass are comparable (Figures 2a and S6).

2.6 | Drivers of the depth distribution of BNPP

We performed a machine learning-based statistical model—random forest (RF)—to explore environmental controls over the depth distribution of BNPP. Before fitting the RF model, variance inflation factor (VIF) (Zuur et al., 2010) was calculated and used to minimize multicollinearity of environmental covariates considered (Table S3). The environmental variables with a VIF value larger than 10 were eliminated in the modelling (Figure S7). To examine how the data spreads throughout the multivariate environmental covariate space and further reduces the dimension of the data, we performed a multiple factor analysis (MFA) using MFA and fviz_mfa_var functions in the R package “FactoMineR”. MFA is an extension of principal component analysis (PCA) for summarizing and visualizing a multivariate data table in which individuals are described by several groups of variables (Figure S8). It takes into account the contribution of all active groups of variables to reveal the most important group of variables that contribute most to explaining the variations in the dataset (Abdi et al., 2013).

To determine the relative importance of selected environmental factors, we calculated the relative contribution of predictor variables to the explained variance (i.e., relative importance) by the model using importance scores for each predictor in the RF model (Figures 3 and S9). Because the RF algorithm inherently performs bagging and random selection of explanatory variables and calculates the out-of-bag error for feature ranking, 500 bootstrap draws from input data were applied to quantify uncertainties in the estimated relative contributions (Grömping, 2009). These assessments were conducted using packages “ranger” and “caret” in R 4.1.2 (R Development Core Team, 2021). We applied partial dependence plots (PDP) from RF modelling results to determine the relationships between predicted depth distribution of BNPP and the most important variables (Figure S9), which accounts for the average effect of one feature on the predicted outcome in the RF model by

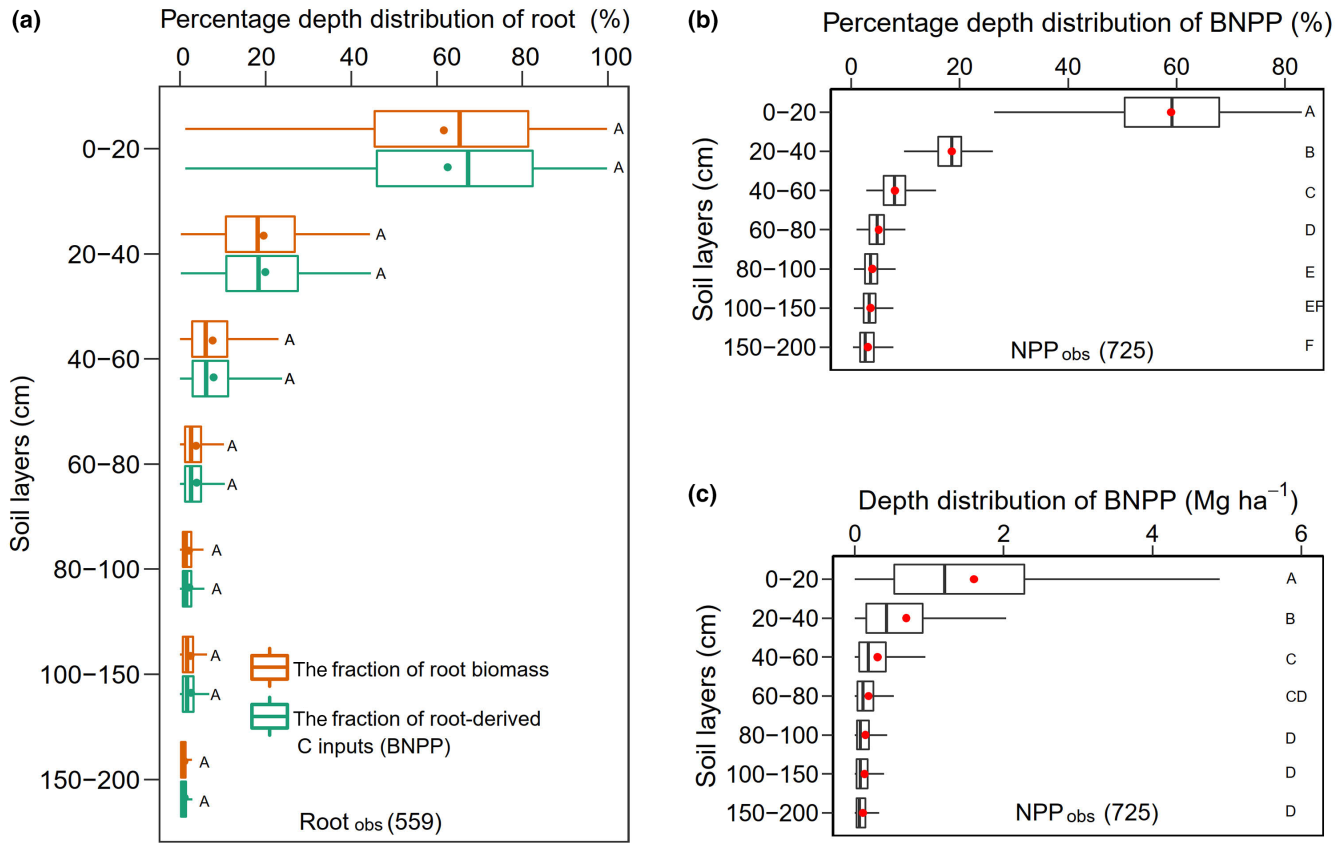

FIGURE 2 Depth distribution of root biomass and belowground net primary productivity (BNPP). (a) The observed proportional depth distribution of root biomass and estimated proportional depth distribution of root inputs from datasets of observed depth distribution of root biomass (Root_{obs}). (b, c) Show the observed proportional depth distribution of BNPP and the observed depth distribution of absolute BNPP among biomes from datasets of observed aboveground and belowground NPP (NPP_{obs}) respectively. Boxplots show the median and interquartile range, with whiskers extending to the most extreme data point which is 1.5×(75%–25%) data range from the box. Significant differences are denoted by different capital letters ($p < 0.05$).

marginalizing other features and show whether the response curves between the target output and a feature is linear, monotonic or more complex (Greenwell, 2017).

2.7 | Global mapping and prediction uncertainties

We explored machine learning-based models (Figure S10), including random forest (RF), extreme gradient boosting (XGBoost), Cubist, support vector machines (SVM), Bayesian regularized artificial neural networks (BRANNs) and lasso regression (LASSO), and selected the best model for predicting BNPP (using NPP_{obs}), the proportional depth distribution of BNPP (PDD, using Root_{obs}) across the globe. For each model, the selected environmental covariates after minimizing multicollinearity via VIF selection and MFA dimensionality reduction were used (see Section 2.6), and 80% of soil profiles in different locations were randomly selected for training, and the remaining 20% for validation. Numeric covariates were standardized with z-scores, and biomes and soil order are categorical variables and were converted into binary variables. The best model tuning parameters (i.e., hyperparameters) were targeted by running the model under a series of parameter combinations using the function “trainControl” in R package “caret”. Specifically, number of trees (num.trees) was set to 500, and the hyperparameters of mtry (number of variables randomly sampled as candidates at each split) and min.node.size (minimum size of terminal nodes) were selected to tune for RF model, eta (learning_rate) and max_depth (maximum depth of a tree) for XGBoost, committees (the number of trees with adjusted weights) and neighbours (the training set which nearest the testing samples) for Cubist, sigma (standard deviation for gaussian kernel) for SVM and neurons (the number of artificial neurons) for BRANNs. The “tuneGrid” method in R package “caret” with 5-fold random cross-validation was used to compute model performance metric (i.e., rooted mean squared error—RMSE) for each model, and the best model with its tuning hyperparameters was targeted with the smallest RMSE.

Using the best model, we predicted BNPP and PDD inferred from roots across the globe with gridded driver variables at a resolution of 0.0083°. BNPP allocated to each soil layer depth was finally calculated as BNPP × PDD. Prediction uncertainty in each 1 km pixel was quantified using a Monte Carlo approach by randomly drawing 500 individual trees with replacement from the random forest model to

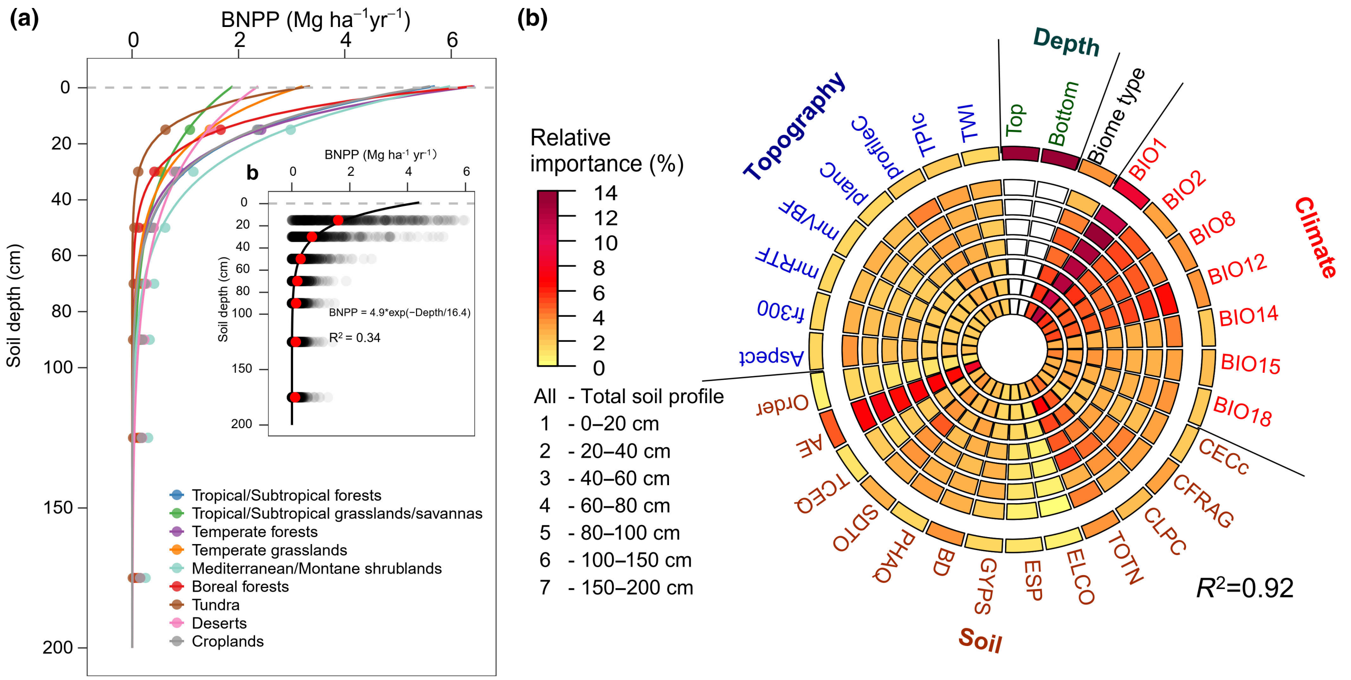

FIGURE 3 Drivers of the depth distribution of belowground net primary productivity (BNPP). (a) The depth distribution of BNPP in nine biomes predicted as an exponential function of soil depth. Dots show biome-specific average BNPP in soil layer depths, and lines show regression lines. Parameters for the regression lines are shown in Table S4. Inset plot in (a) shows the relationship pooling all data together, with red dots show global averages. (b) The relative importance of environmental factors for predicting BNPP depth distribution using a random forest model. The outer ring shows results for the whole soil profile, and the seven inner rings show results for seven soil layer depths respectively. See Table S3 for the details of the environmental predictors.

predict BNPP and PDD. These 500 estimates were used to calculate the mean (*m*) and standard deviation (*sd*) of BNPP and PDD at each of the seven-layer depths. The prediction uncertainty (*U*) was expressed as the coefficient of variation (CV), that is, $U = sd/m$. The total uncertainty of depth-specific BNPP (BNPP × PDD, Figure S11) was estimated as $U_{total} = \sqrt{U^2_{BNPP} + U^2_{PDD}}$.

To assess the quality of global maps, we further estimated BNPP using RF models with spatial cross-validation. Spatial cross-validation aimed at creating independence between cross-validation folds to overcome potential uncertainties caused by spatial autocorrelation (which is very common for clustered dataset) (Meyer et al., 2018; Meyer & Pebesma, 2022). For model training, we used CreateSpacetimeFolds function in the R package “CAST” to create five independent folds for spatial cross-validation followed the approach of Meyer and Pebesma (2021). In addition, we also calculated dissimilarity index (DI, an index of standardize distance in predictor space for new location) and area of applicability (AOA, which is designed to analyse if the model can be applied to the entire study area or if there are locations that are very different in their predictor properties to what the model has been trained) to illustrate the area where our prediction model (both with random and spatial cross-validation) can be reliably applied. By applying the model to the data, we indeed found that the model performed better in AOA than outside AOA. Since DI can quantitatively express prediction uncertainty, we estimated DI using “aoa” function in the R package “CAST” in AOA and in the area outside AOA across the globe. Finally, we compared the global mapping products using random cross-validation and spatial cross-validation predictions.

3 | RESULTS

3.1 | The total amount of BNPP

Averaging across the 725 NPP_{obs} soil profiles (Figure 1a), BNPP allocated to the 0–200 cm soil profile was 3.28 (0.19, 12.0) Mg ha^{-1} yr^{-1} (mean with 2.5% and 97.5% quantiles, Figure 1b) and significantly different among biomes ($p < 0.05$; Figure 1b). Mediterranean/montane shrublands had the highest BNPP of 5.49 (2.68, 15.2) Mg ha^{-1} yr^{-1}, followed by croplands of 4.42 (1.05, 17.0) Mg ha^{-1} yr^{-1} and tropical/subtropical forests of 4.29 (1.92, 13.3) Mg ha^{-1} yr^{-1}, and tundra had the lowest of 0.9 (0.24, 3.41) Mg ha^{-1} yr^{-1} (Figure 1b). The fraction of NPP allocated belowground (i.e., f_{BNPP}) was 38% (8%, 83%) with significant differences among biomes (Figure 1c). It was on average greater than 50% in arid and semi-arid environments such as temperate grasslands and deserts, but only ~30% in tropical/subtropical, temperate and boreal forests (Figure 1c).

3.2 | The depth distribution of BNPP

Using the two-pool root turnover model, no significant difference between the proportional depth distribution of root biomass and BNPP was found across the globe as well as among biomes (Figures 2a and S6). On average, ~60% of BNPP was allocated to the 0–20 cm soil layer (Figure 2b); and ~80% to the top 40 cm soil layer (Figure 2b). In other deeper soil layers, BNPP was relatively small and showed much less variance than in upper layers (Figure 2b). In the top 20 cm soil layer, for example, PDD ranged from 37% (2.5% quantile) to 78% (97.5% quantile). For PDD in a soil layer depth, it was significantly ($p<0.05$) different among biomes (Figure 2c). Boreal forests and tundra allocated more BNPP (~70%) to upper layers (e.g., 0–20 cm) than other biome types (e.g., <50% in tropical/subtropical grasslands/savannas and deserts which allocate more BNPP to deeper layer depths, Figure S5).

Similar to PDD (Figure 2a), the absolute amount of BNPP was decreased exponentially with soil, with greater variances in upper soil layers than in deeper layers. Across the globe, the average BNPP was estimated to be 1.60 Mg ha^{-1} yr^{-1} in the top 20 cm soil (Figure 2c). In the 20–40 cm soil layer, the average was reduced to 0.69 Mg ha^{-1} yr^{-1}. In deeper layers, it was relatively small and comparable (<0.30 Mg ha^{-1} yr^{-1}) with smaller variances (Figure 2c). Among biomes, absolute BNPP showed significant disparities (Figure 2c). In upper layers (e.g., 0–20 cm), higher BNPP was observed in Mediterranean/montane shrublands (2.37 Mg ha^{-1} yr^{-1}) and temperate forests (2.11 Mg ha^{-1} yr^{-1}) than in boreal forests (0.94 Mg ha^{-1} yr^{-1}) and tundra (0.52 Mg ha^{-1} yr^{-1}). In deeper soil layers, the variations in absolute BNPP among biomes were in general consistent with those in the top 0–20 cm soil (Figure S5).

3.3 | Drivers of BNPP across soil layers

As expected, soil depth was the most important predictor for the depth distribution of BNPP (Figure 3a,b). An exponential model using depth as the only predictor explained 23%–56% of the variance in the depth distribution of BNPP across the globe ($R^2=0.34$) and in different biome types (R^2 ranged from 0.23 to 0.56; Figure 3a, Table S4). The coefficients of the exponential model, which indicate the decreasing rate of BNPP with soil depth, were significantly different among biomes (Table S4), demonstrating that the depth distribution of BNPP is significantly different among biomes (Figure 2).

The random forest model taking into account soil depth, biome and 55 environmental covariates (Table S3), after controlling for multicollinearity among the covariates (Figures S7 and S8), explained 92% ($R^2=0.92$) of the variance in the depth distribution of BNPP in the whole 0–200 cm soil profile (Figure 3b). Following soil depth, mean annual temperature, mean actual daily soil evaporation, biome, soil bulk density and mean annual precipitation were the five most important predictors (Figure 3b). Grouping environmental predictors into climatic (temperature- and precipitation-related, a total of 7 variables), edaphic (12 variables) and topographic (7 variables) variables, the result indicated that the contributions of climate, soil and topography to explained variance were 26%, 28% and 13% respectively (Table S5). Focusing on BNPP in specific soil layer depths, the fitted random forest models explained over 80% of its variance in each of the seven soil layers (Figure S9). BIO1 (mean annual temperature) was consistently the most important factor, followed by AE (actual mean daily soil evaporation), BIO12 (mean annual precipitation) and TOTN (total soil nitrogen content) in deeper layers (Figures 3b and S9). In terms of the overall influence of climatic, edaphic and topographic variables, climatic variables contributed 33%–40%; and edaphic and topographic properties contributed 33%–40% and 18%–28% respectively (Figures 3b and S9; Table S5). For the five most important predictors for each layer, nonlinear relationships with BNPP were detected (Figure S9). In general, predictors exhibited positive effects on BNPP. For example, BIO1, which was the most important climate variable for all soil layers, positively influences BNPP until saturating at higher values of BIO1. At the lower range of TOTN, TOTN exhibited a positive and then a negative relationship with BNPP (Figure S9).

3.4 | Global patterns of the depth distribution of BNPP

The depth distribution of BNPP was mapped across the globe at 0.0083° resolution (Figure 4) using the best ML model with random cross-validation (random forest was consistently the best model; Figures S4 and S10). Across the globe, BNPP in the 0–200 cm soil profile was 2.00 (0.41, 3.95) Mg ha^{-1} yr^{-1} (Figures 4 and 5a). The largest BNPP on average occurred in ~20° N (Figure 5a). In all soil layers, BNPP was relatively low in deserts and high latitudinal regions of the northern Hemisphere (Figure 4) with an apparent decreasing trend from 40° N to 80° N (Figure 5a). The highest BNPP was in tropical/subtropical forests, temperate forests and croplands; and the lowest in tundra, boreal forests and deserts (Figure 4). For the proportional depth distribution, averaging across the globe, it was 57% and 77% in the top 20 and 40 cm soil layers respectively (Figure 5b). With increasing latitudes from 40° N to 80° N, more BNPP was allocated to upper soil layers (Figure 5b). Figure S11 shows the uncertainty (i.e., coefficient of variance in each 1 km grid) in predicted depth-specific BNPP. The uncertainty was greater in deeper soil layers, particularly in the northern Hemisphere high latitudinal regions such as tundra and boreal forests. Indeed, the uncertainty was markedly higher in tundra and boreal forests than in other biomes in deeper soil

FIGURE 4 Global pattern of belowground net primary productivity (BNPP) to seven soil layers (left panel) with the corresponding aggregated BNPP in nine biomes (right panel). Boxplots show the median and interquartile range with whiskers extending to 1.5 times of the interquartile range. Red dots and blue dash lines show biome-specific and global averages respectively. Significant differences in BNPP among biomes in a typical soil layer are denoted by different capital letters ($p<0.05$). Please note the different scales in different depths.

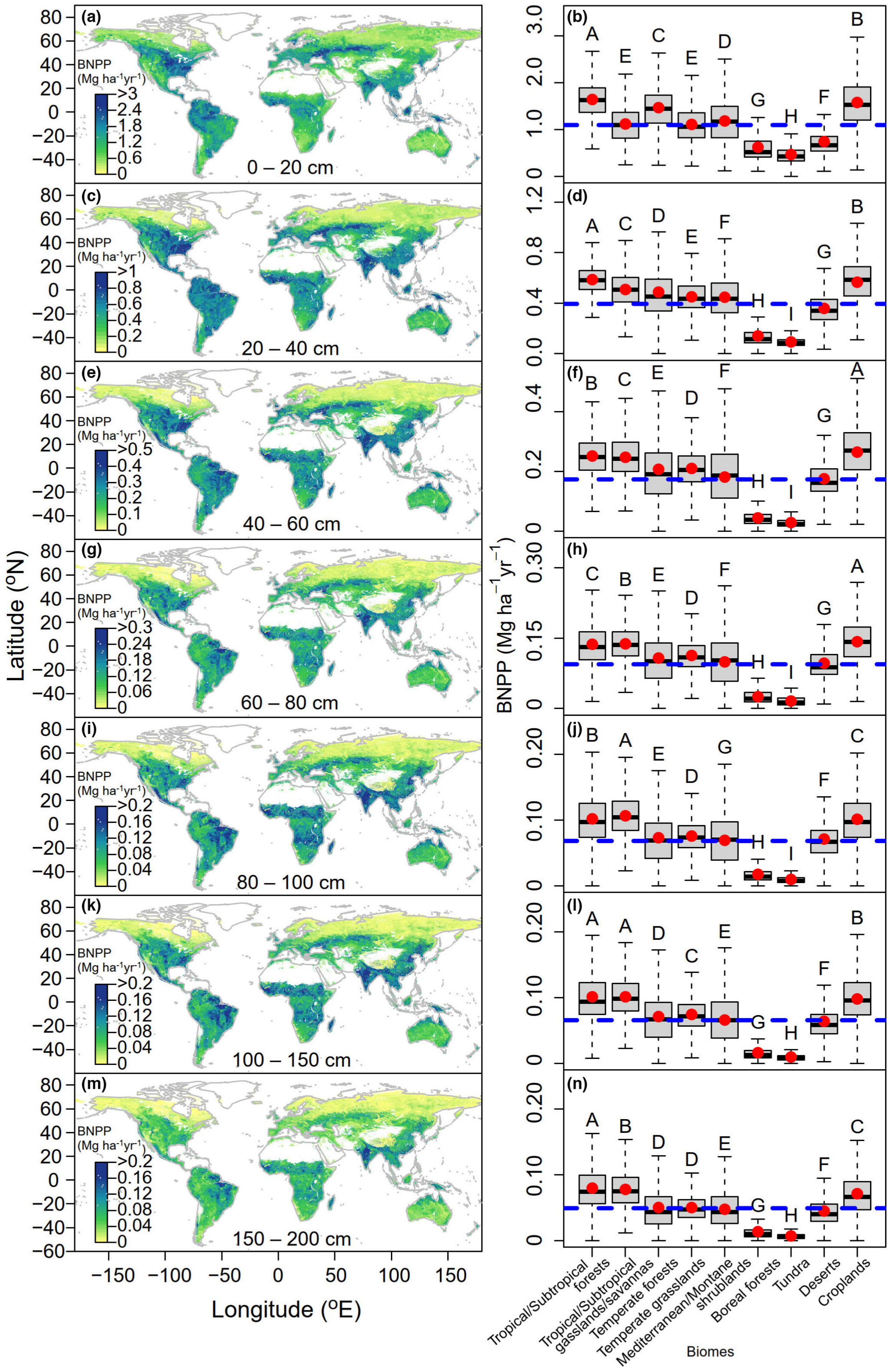
(a)
BNPP (Mg ha-1yr-1)
>3
2.4
1.8
1.2
0.6
0
0 – 20 cm
(c)
>1
0.8
0.6
0.4
0.2
0
20 – 40 cm
(e)
>0.5
0.4
0.3
0.2
0.1
0
40 – 60 cm
(g)
>0.3
0.24
0.18
0.12
0.06
0
60 – 80 cm
(i)
>0.2
0.16
0.12
0.08
0.04
0
80 – 100 cm
(k)
100 – 150 cm
(m)
150 – 200 cm
Latitude (oN)
Longitude (oE)
80
60
40
20
0
−20
−40
−60
−150
−100
−50
0
50
100
150
(b)
A E C E D G H F B
(d)
A C D E F H I G B
(f)
B C E D F H I G A
(h)
C B E D F H I G A
(j)
B A E D G H I F C
(l)
A A D C E G H F B
(n)
A B D D E G H F C
BNPP (Mg ha−1 yr−1)
Tropical/Subtropical forests
Tropical/Subtropical gasslands/savannas
Temperate forests
Temperate grasslands
Mediterranean/Montane shrublands
Boreal forests
Tundra
Deserts
Croplands
Biomes

layers. Across the globe, the average uncertainty in the top 20 cm layer was 0.48 (0.27, 0.72), and increased to 1.90 (0.89, 4.28) in the 150–200 cm layer (Figure S11).

By applying a RF model with spatial cross-validation to the data, we found that the model performed better in AOA areas than in areas outside AOA (Figure S12b,c). Figure 6 compares global DI (dissimilarity index) distribution pattern estimated using random and spatial cross-validation. The area outside AOA derived from the model with random cross-validation (18%) was larger than that with spatial cross-validation (2%), mainly located in South America, Africa, Australia and Western China. However, in both AOA and outside AOA areas, the predictions of the two validation approaches

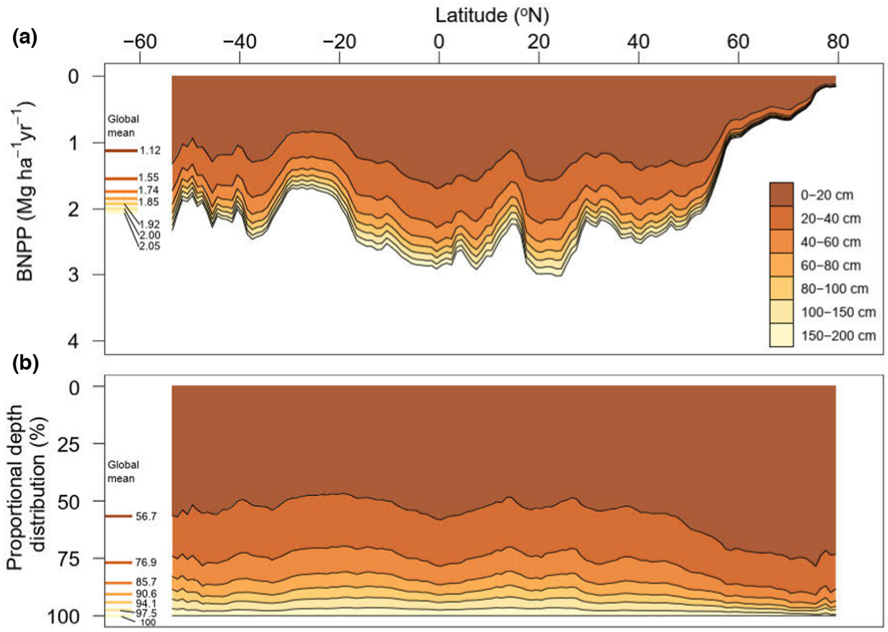

FIGURE 5 Latitudinal pattern of belowground net primary productivity (BNPP). (a) Depth distribution of absolute BNPP; (b) proportional depth distribution of BNPP. Both absolute and proportional BNPP were calculated based on aggregated BNPP and its depth distribution in each 1 degree of latitude. Bars and the relevant numbers beside the left *y*-axes indicate the global cumulative average with increasing soil depths.

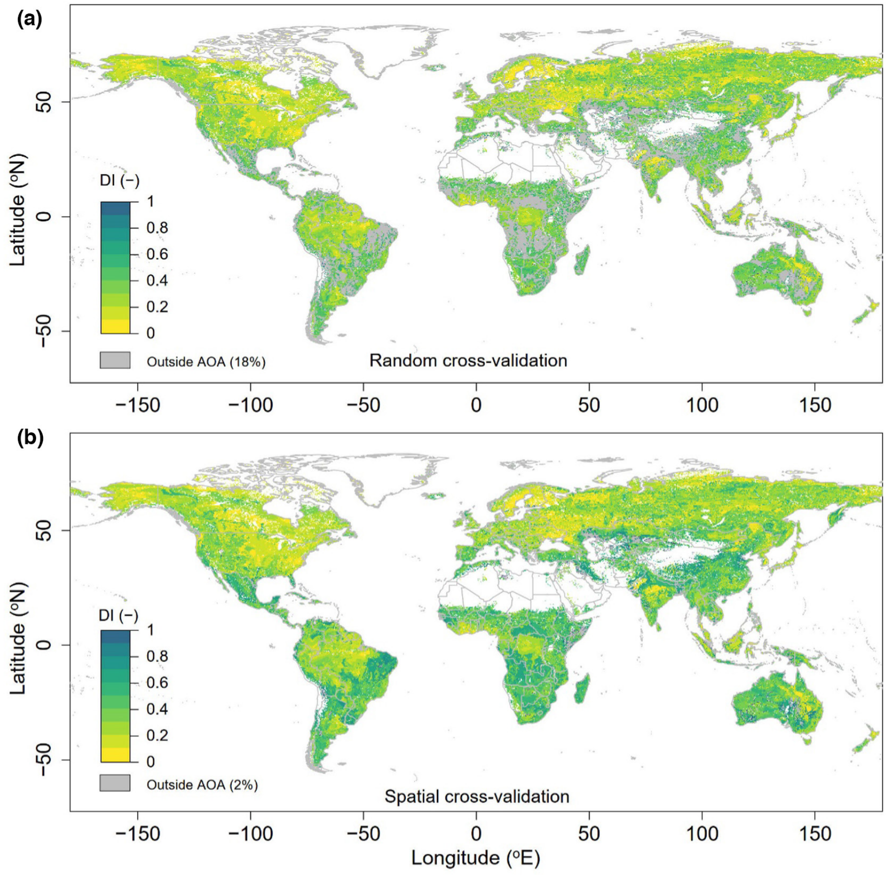

FIGURE 6 Global pattern of dissimilarity index (DI) and the area outside of applicability (Outside AOA) derived from random forest models with random cross-validation (a) and spatial cross-validation (b). DI is a standardized distance for new prediction locations used for quantitatively expressing prediction uncertainty. The area of applicability (AOA) is the area where the model is trained, and where the cross-validation performance holds. If DI is larger than a DI threshold (which is determined by the DI values from the cross-validated training data), the new data point falls outside the AOA.

were similar (the difference of RMSE was no more than 0.18 g m^{-2}, Figure S13). Overall, these additional results validate the random cross-validation approach for estimating BNPP.

4 | DISCUSSION AND CONCLUSIONS

Using root biomass profiles to infer the depth distribution of BNPP, we generated field observational data-derived global maps of BNPP down to 200 cm at a resolution of ~1 km. In the 0–200 cm soil profile, global average BNPP is estimated to be ~2 Mg ha^{-1} yr^{-1} with a global total BNPP of ~21 Pg yr^{-1}. This estimate is close to the value of 2.2 Mg ha^{-1} yr^{-1} (with a global total belowground carbon fixation of 24.7 Pg yr^{-1}) estimated by Gherardi and Sala (2020) who estimated total BNPP as the difference between satellite-derived NPP and field measurements of aboveground NPP. Among biomes, BNPP in forests, grasslands and shrublands/savannas are estimated to be 2.7, 2.0 and 2.2 Mg ha^{-1} yr^{-1}, respectively, which are also close to the values estimated by Gherardi and Sala (2020).

The majority of BNPP (~60%) is allocated to the top 20 cm soil layer, and an additional ~20% to the 20–40 cm soil layer. This is consistent with field observations of BNPP depth distribution at individual sites across the globe (Hertel et al., 2009; López-Mársico et al., 2015; Xu et al., 2014). Among biomes, however, the depth distribution of BNPP is significantly different. Generally, more BNPP is allocated to deeper layers in drier biomes (e.g., deserts and grasslands). This may be due to the close coupling of plant root growth with soil moisture profiles (Fan et al., 2017; Lambers & Oliveira, 2019). More assimilated carbon would be allocated to deeper layers in drier environments to acquire water (Ledo et al., 2018; Mokany et al., 2006). A synthesis of literature data has found that tropical grasslands/savannas and deserts have the deepest rooting depth compared with other biomes (Canadell et al., 1996). There is also a clear pattern of higher allocation of BNPP to upper layers in higher latitudes. Due to low temperature in high latitudinal regions, deep soil permafrost (e.g., in tundra) would persist during the growing season, inhibiting root growth in the subsoil (Blume-Werry et al., 2019; Canadell et al., 1996; Jackson et al., 1996). As a result, a large fraction of BNPP would allocate to surface layers. As biome is inherently determined by climate, it is reasonable to expect that climatic factors play a key role in regulating the depth distribution of BNPP. In addition, we note that BNPP in deeper soil layers is relatively small and shows much less variance than in upper layers. This result is consistent with carbon isotope-based estimates of carbon inputs to deeper soil depths (Balesdent et al., 2018). Except the increasing penetration resistance of root growth to deep layers, another reason may be that topsoil is subject to more frequent fluctuations in soil environmental properties (e.g., soil temperature, moisture and nutrient availability) than the subsoil, and a greater soil volume in deeper layers would buffer soil environmental conditions to a large extent, resulting in relatively large variability of BNPP in the topsoil.

As expected, climatic variables have significant effects on BNPP and its depth distribution. Mean annual temperature (BIO1) and precipitation (BIO12) are identified to be the most important. BIO12 is the predominant source of soil moisture; while BIO1 determines the loss rate of soil moisture via evaporation and plant transpiration and the depth of active layer above the permafrost. Previous assessments at broad scales mainly focused on BIO1 and BIO12, and have demonstrated the importance of these two climatic variables (Gherardi & Sala, 2020; Gill et al., 2002; Girardin et al., 2010). Our result further confirms the dominant role of climatic drivers in BNPP depth allocation. However, previous studies have found that the degree and even the direction of the correlation of BNPP with BIO1 and BIO12 are biome-dependent (Reich et al., 2018; Walker et al., 2006). This may be attributed to the differential responses of biomes to temperature and precipitation shifts depending on plant functional types and carbon allocation strategies (Wang et al., 2012; Way & Oren, 2010). For example, the growth of tropical species is more vulnerable to high temperature or drought than temperate or boreal trees (Way & Oren, 2010). We found that there was little difference in the response curve of BNPP to BIO1 and BIO12 in different soil depth (Figure S9).

Except for BIO1 and BIO12, other climatic variables associated with climate seasonality and inter-annual variability also play a role in regulating the depth distribution of BNPP. Mean temperature diurnal range (i.e., BIO2) and mean temperature of the wettest quarter (i.e., BIO8) are the most important climatic variables after BIO1 and BIO12 (Figures 3b and S9). Overall, these results suggest that both the mean and variability of climatic conditions are important determinants of belowground plant carbon allocation; and, more importantly, the direction and magnitude of their effects are biome-specific probably depending on local plant functional types and their response to soil water regimes. Future climate (e.g., warming and precipitation change) and land cover changes (e.g., vegetation shift) may significantly alter the amount of BNPP allocated to different soil layer depths, thereby potentially modifying biogeochemical processes (e.g., soil carbon balance and greenhouse gas emissions) across soil depths that are regulated by fresh carbon inputs.

Despite the leading role of climate, soil physicochemical properties also play a vital role in soil BNPP variation across space. Indeed, mean actual daily soil evaporation (which is affected by both soil properties and climatic conditions) is as important as BIO1 and BIO12, positively influencing BNPP (Figure S9), in line with the findings for global grasslands (Sun et al.,2021). A major reason would be that high soil evaporation means a higher probability of water stress, given otherwise similar environmental conditions. Total soil nitrogen content as an indicator of soil nutrient availability also exerts a positive effect, particularly in deeper layers (Figure 3b,c). Together with the general positive relationship between BNPP and climatic variables, these results reflect the key role of energy (e.g., temperature) and soil resource profiles (e.g., water, nitrogen and other nutrients) in regulating the depth distribution of BNPP. More accurate depth-resolved information of soil resources that directly influence plant growth, particularly soil nutrient availability, would promote a more reliable prediction of BNPP and its depth allocation (Vicca et al., 2018). Soil physical properties also cannot be ignored.

For example, both soil bulk density and sand show negative effects. They are key soil physical parameters determining the suitability of soil environment for root growth (Dexter, 2004). Another noteworthy phenomenon is that the effect of a specific soil property is soil layer-dependent, while the layer dependence of the effects of climatic and topographic variables is much weaker (Figure S9). These results demonstrate that the depth distribution of BNPP is driven by complex interplay among edaphic, climatic and topographic variables, which is further modulated by biome type as different biomes may adopt distinct carbon allocation strategies (Malhi et al., 2017; McCarthy et al., 2010; Wieder et al., 2015).

The data used in this study build upon quality-checked legacy datasets, and we further updated the data via literature synthesis to generate a more comprehensive one that improves spatial coverage and benefits robust assessment at the global scale. Although we show evidence that the two datasets are not statistically different in terms of BNPP estimates (derived from peer-reviewed publications vs. the ORNL DAAC legacy data; Figure S3), here we note several limitations in the estimation of root-derived BNPP due to the difficulty in field measurements and assumptions (Clark et al., 2001; Milchunas & Lauenroth, 2001). First, not all data include all BNPP components such as root exudates. BNPP allocated to root exudates and mycorrhizae may account for a considerable fraction of BNPP (particularly in forests) but is challenging to measure them in situ (Bertin et al., 2003; Clark et al., 2001). As such, BNPP would be underestimated and depend on the approach used to measure BNPP. Second, most data only include BNPP in a single year, but BNPP varies across years. Given that we focus on the spatial variability of BNPP across the globe, however, the consequences of temporal variability on our estimates would be small if we accept that interannual variability is smaller than spatial variability across the globe. Third, our approach implicitly assumes that roots in different soil depths have the same turnover times. For some plants, roots in different soil layers (e.g., coarse vs. fine roots) may have different functions, and roots with different functions may distribute unequally in soil layer depths (Freschet et al., 2017; Jackson et al., 1996). Thus, turnover times of different root functional types may be different, resulting in biases in the estimation of the proportional depth distribution of carbon inputs according to root biomass alone. However, our simulations using a two-pool root turnover model did not find differences between the vertical distributions of BNPP and root biomass (Figure 2a). Fourth, different approaches could be adopted to measure BNPP in different studies and can potentially cause uncertainties in the estimation. In the 54 literatures used for BNPP data collection in this study (Appendix A—Data sources), soil cores (22 papers) and ingrowth cores (26 papers) are the two most common approaches. We found that across most biomes, BNPP observed using different approaches (e.g., soil cores vs. ingrowth cores) are comparable (Figure S2), although discrepancies between datasets were found in several ecosystems, particularly in tundra ecosystems, possibly due to limited data availability. Thus, the uncertainties caused by different approaches to quantify BNPP would be small (Makkonen & Helmisaari, 1999). However, we acknowledge that BNPP measured using other approaches such as minirhizotron and isotope labelling may be significantly different from those using soil cores and ingrowth cores (Kuzyakov & Schneckenberger, 2004; Milchunas, 2009). In addition, for global BNPP mapping, it should be noted that soil depth would not reach to 2 m. Thus, our estimation of 0–2 m soil profile would be an overestimation of overall BNPP in some regions with shallow soils. Overall, we need a cost-efficient technique that can be easily applied across different biomes to accurately measure depth-resolved BNPP in situ.

To our knowledge, we are the first to spatially explicitly predict depth-specific BNPP across the globe using consistent approaches with the quantification of prediction uncertainties, and demonstrate the vital role of climatic and edaphic variables in controlling the distribution of BNPP across the globe as well as along the soil profile. The quantitative information is critical for explicit representation of soil layer-specific carbon inputs. By quantifying the spatial pattern of the depth distribution of carbon inputs, our maps provide information on belowground plant carbon allocation across the globe, which can be used to parameterize, scale or benchmark spatially explicit modelling of carbon cycle and facilitate more reliable predictions of whole-profile soil carbon dynamics across biomes as well as across the globe.

AUTHOR CONTRIBUTIONS

Zhongkui Luo conceived the study. Guocheng Wang, Liujun Xiao, Zhongkui Luo, Jinfeng Chang, Yaoyao Chen and Lei Cheng compiled the data. Liujun Xiao, Guocheng Wang and Zhongkui Luo led the data assessment with the contributions of Xiali Mao and Xiaowei Guo Liujun Xiao conducted global mapping. Zhongkui Luo, Liujun Xiao, Guocheng Wang, Mingming Wang, Shuai Zhang, Zhou Shi, Yiqi Luo, Kailiang Yu and Fei Mo interpreted the results with the contribution of all authors. Zhongkui Luo, Liujun Xiao and Guocheng Wang led manuscript writing with substantial contributions of all authors.

ACKNOWLEDGEMENTS

We acknowledge financial support from the national key research program of the Ministry of Science and Technology of China (grant no. 2021YFE0114500) and the National Natural Science Foundation of China (Grant Nos. 42001105, 32171639, 32241036) and State Key Laboratory of Atmospheric Boundary Layer Physics and Atmospheric Chemistry (LAPC-KF-2022-10).

CONFLICT OF INTEREST STATEMENT

The authors declare that they have no conflict of interest.

DATA AVAILABILITY STATEMENT

Data, code and digital maps of BNPP generated in this study can be accessed from: https://figshare.com/articles/dataset/Datasets_of_NPP_soil_radiocarbon_and_root_biomass/12840050.

ORCID

Liujun Xiao https://orcid.org/0000-0002-1900-1586
Zhongkui Luo https://orcid.org/0000-0002-6744-6491

REFERENCES

Abatzoglou, J. T., Dobrowski, S. Z., Parks, S. A., & Hegewisch, K. C. (2018). TerraClimate, a high-resolution global dataset of monthly climate and climatic water balance from 1958-2015. *Scientific Data*, *5*, 170191.

Abdi, H., Williams, L. J., & Valentin, D. (2013). Multiple factor analysis: Principal component analysis for multitable and multiblock data sets. *Wiley Interdisciplinary Reviews: Computational Statistics*, *5*(2), 149–179.

Amatulli, G., Domisch, S., Tuanmu, M.-N., Parmentier, B., Ranipeta, A., Malczyk, J., & Jetz, W. (2018). A suite of global, cross-scale topographic variables for environmental and biodiversity modeling. *Scientific Data*, *5*(1), 180040. https://doi.org/10.1038/sdata.2018.40

Balesdent, J., Basile-Doelsch, I., Chadoeuf, J., Cornu, S., Derrien, D., Fekiacova, Z., & Hatté, C. (2018). Atmosphere–soil carbon transfer as a function of soil depth. *Nature*, *559*(7715), 599–602.

Batjes, N. H. (2016). Harmonized soil property values for broad-scale modelling (WISE30sec) with estimates of global soil carbon stocks. *Geoderma*, *269*, 61–68.

Bertin, C., Yang, X., & Weston, L. A. (2003). The role of root exudates and allelochemicals in the rhizosphere. *Plant and Soil*, *256*(1), 67–83.

Blume-Werry, G., Milbau, A., Teuber, L. M., Johansson, M., & Dorrepaal, E. (2019). Dwelling in the deep–strongly increased root growth and rooting depth enhance plant interactions with thawing permafrost soil. *New Phytologist*, *223*(3), 1328–1339.

Camino-Serrano, M., Guenet, B., Luyssaert, S., Ciais, P., Bastrikov, V., De Vos, B., Gielen, B., Gleixner, G., Jornet-Puig, A., Kaiser, K., Kothawala, D., Lauerwald, R., Peñuelas, J., Schrumpf, M., Vicca, S., Vuichard, N., Walmsley, D., & Janssens, I. A. (2018). ORCHIDEE-SOM: Modeling soil organic carbon (SOC) and dissolved organic carbon (DOC) dynamics along vertical soil profiles in Europe. *Geoscientific Model Development*, *11*(3), 937–957.

Canadell, J., Jackson, R. B., Ehleringer, J. B., Mooney, H. A., Sala, O. E., & Schulze, E. D. (1996). Maximum rooting depth of vegetation types at the global scale. *Oecologia*, *108*(4), 583–595.

Channan, S., Collins, K., & Emanuel, W. (2014). *Global mosaics of the standard MODIS land cover type data*. University of Maryland and the Pacific Northwest National Laboratory.

Cheng, W. X., Parton, W. J., Gonzalez-Meler, M. A., Phillips, R., Asao, S., McNickle, G. G., Brzostek, E., & Jastrow, J. D. (2014). Synthesis and modeling perspectives of rhizosphere priming. *New Phytologist*, *201*(1), 31–44.

Clark, D. A., Brown, S., Kicklighter, D. W., Chambers, J. Q., Thomlinson, J. R., & Ni, J. (2001). Measuring net primary production in forests: Concepts and field methods. *Ecological Applications*, *11*(2), 356–370.

Conrad, O., Bechtel, B., Bock, M., Dietrich, H., Fischer, E., Gerlitz, L., Wehberg, J., Wichmann, V., & Böhner, J. (2015). System for automated geoscientific analyses (SAGA) v. 2.1.4. *Geoscientific Model Development*, *8*(7), 1991–2007. https://doi.org/10.5194/gmd-8-1991-2015

Cramer, W., Bondeau, A., Woodward, F. I., Prentice, I. C., Betts, R. A., Brovkin, V., Cox, P. M., Fisher, V., Foley, J. A., Friend, A. D., Kucharik, C., Lomas, M. R., Ramankutty, N., Sitch, S., Smith, B., White, A., & Young-Molling, C. (2001). Global response of terrestrial ecosystem structure and function to CO_2 and climate change: Results from six dynamic global vegetation models. *Global Change Biology*, *7*(4), 357–373.

Davidson, E. A., Savage, K., Bolstad, P., Clark, D. A., Curtis, P. S., Ellsworth, D. S., Hanson, P. J., Law, B. E., Luo, Y., Pregitzer, K. S., Randolph, J. C., & Zak, D. (2002). Belowground carbon allocation in forests estimated from litterfall and IRGA-based soil respiration measurements. *Agricultural and Forest Meteorology*, *113*(1), 39–51.

Dexter, A. R. (2004). Soil physical quality: Part I. theory, effects of soil texture, density, and organic matter, and effects on root growth. *Geoderma*, *120*(3), 201–214. https://doi.org/10.1016/j.geoderma.2003.09.004

Fan, N., Koirala, S., Reichstein, M., Thurner, M., Avitabile, V., Santoro, M., Ahrens, B., Weber, U., & Carvalhais, N. (2020). Apparent ecosystem carbon turnover time: Uncertainties and robust features. *Earth System Science Data Discussions*, *2020*, 1–25.

Fan, Y., Miguez-Macho, G., Jobbágy, E. G., Jackson, R. B., & Otero-Casal, C. (2017). Hydrologic regulation of plant rooting depth. *Proceedings of the National Academy of Sciences of the United States of America*, *114*(40), 10572–10577.

Fick, S. E., & Hijmans, R. J. (2017). WorldClim 2: New 1-km spatial resolution climate surfaces for global land areas. *International Journal of Climatology.*, *37*, 4302–4315.

Freschet, G. T., Valverde-Barrantes, O. J., Tucker, C. M., Craine, J. M., McCormack, M. L., Violle, C., Fort, F., Blackwood, C. B., Urban-Mead, K. R., Iversen, C. M., Bonis, A., Comas, L. H., Cornelissen, J. H. C., Dong, M., Guo, D., Hobbie, S. E., Holdaway, R. J., Kembel, S. W., Makita, N., … Roumet, C. (2017). Climate, soil and plant functional types as drivers of global fine-root trait variation. *Journal of Ecology*, *105*(5), 1182–1196.

Friedlingstein, P., Cox, P., Betts, R., Bopp, L., Von Bloh, W., Brovkin, V., Cadule, P., Doney, S., Eby, M., Fung, I., Bala, G., John, J., Jones, C., Joos, F., Kato, T., Kawamiya, M., Knorr, W., Lindsay, K., Matthews, H. D., … Zeng, N. (2006). Climate-carbon cycle feedback analysis: Results from the (CMIP)-M-4 model intercomparison. *Journal of Climate*, *19*(14), 3337–3353.

Garnier, E. (1991). Resource capture, biomass allocation and growth in herbaceous plants. *Trends in Ecology & Evolution*, *6*(4), 126–131.

Gherardi, L. A., & Sala, O. E. (2020). Global patterns and climatic controls of belowground net carbon fixation. *Proceedings of the National Academy of Sciences of the United States of America*, *117*, 202006715.

Gill, R. A., Kelly, R. H., Parton, W. J., Day, K. A., Jackson, R. B., Morgan, J. A., Scurlock, J. M. O., Tieszen, L. L., Castle, J. V., Ojima, D. S., & Zhang, X. S. (2002). Using simple environmental variables to estimate belowground productivity in grasslands. *Global Ecology and Biogeography*, *11*(1), 79–86. https://doi.org/10.1046/j.1466-822X.2001.00267.x

Girardin, C. A. J., Malhi, Y., Aragão, L. E. O. C., Mamani, M., Huaraca Huasco, W., Durand, L., Feeley, K. J., Rapp, J., Silva-Espejo, J. E., Silman, M., Salinas, N., & Whittaker, R. J. (2010). Net primary productivity allocation and cycling of carbon along a tropical forest elevational transect in the Peruvian Andes. *Global Change Biology*, *16*(12), 3176–3192.

Green, J. K., Seneviratne, S. I., Berg, A. M., Findell, K. L., Hagemann, S., Lawrence, D. M., & Gentine, P. (2019). Large influence of soil moisture on long-term terrestrial carbon uptake. *Nature*, *565*(7740), 476–479.

Greenwell, B. M. (2017). Pdp: An R package for constructing partial dependence plots. *The R Journal*, *9*(1), 421.

Greiner, L., Keller, A., Grêt-Regamey, A., & Papritz, A. (2017). Soil function assessment: Review of methods for quantifying the contributions of soils to ecosystem services. *Land Use Policy*, *69*, 224–237.

Grömping, U. (2009). Variable importance assessment in regression: Linear regression versus random forest. *The American Statistician*, *63*(4), 308–319.

Hertel, D., Moser, G., Culmsee, H., Erasmi, S., Horna, V., Schuldt, B., & Leuschner, C. (2009). Below- and above-ground biomass and net primary production in a paleotropical natural forest (Sulawesi, Indonesia) as compared to neotropical forests. *Forest Ecology and Management*, *258*(9), 1904–1912. https://doi.org/10.1016/j.foreco.2009.07.019

Imhoff, M. L., Bounoua, L., Ricketts, T., Loucks, C., Harriss, R., & Lawrence, W. T. (2004). Global patterns in human consumption of net primary production. *Nature*, *429*(6994), 870–873.

Jackson, R., Canadell, J., Ehleringer, J. R., Mooney, H., Sala, O., & Schulze, E. D. (1996). A global analysis of root distributions for terrestrial biomes. *Oecologia*, *108*(3), 389–411.

Schenk, H. J., & Jackson, R. B. (2002). The global biogeography of roots. *Ecological Monographs*, *72*(3), 311–328. https://doi.org/10.1890/0012-9615(2002)072[0311:TGBOR]2.0.CO;2

Krausmann, F., Erb, K.-H., Gingrich, S., Haberl, H., Bondeau, A., Gaube, V., Lauk, C., Plutzar, C., & Searchinger, T. D. (2013). Global human appropriation of net primary production doubled in the 20th century. *Proceedings of the National Academy of Sciences of the United States of America*, *110*(25), 10324–10329.

Kuzyakov, Y. (2010). Priming effects: Interactions between living and dead organic matter. *Soil Biology & Biochemistry*, *42*(9), 1363–1371.

Kuzyakov, Y., & Schneckenberger, K. (2004). Review of estimation of plant rhizodeposition and their contribution to soil organic matter formation. *Archives of Agronomy and Soil Science*, *50*(1), 115–132.

Lambers, H., & Oliveira, R. S. (2019). Plant water relations. In *Plant physiological ecology* (pp. 187–263). Springer.

Le Quéré, C., Andrew, R. M., Friedlingstein, P., Sitch, S., Pongratz, J., Manning, A. C., Korsbakken, J. I., Peters, G. P., Canadell, J. G., Jackson, R. B., Boden, T. A., Tans, P. P., Andrews, O. D., Arora, V. K., Bakker, D. C. E., Barbero, L., Becker, M., … Zhu, D. (2018). Global carbon budget 2017. *Earth System Science Data*, *10*(1), 405–448.

Ledo, A., Paul, K. I., Burslem, D. F. R. P., Ewel, J. J., Barton, C., Battaglia, M., Brooksbank, K., Carter, J., Eid, T. H., England, J. R., Fitzgerald, A., Jonson, J., Mencuccini, M., Montagu, K. D., Montero, G., Mugasha, W. A., Pinkard, E., Roxburgh, S., Ryan, C. M., … Chave, J. (2018). Tree size and climatic water deficit control root to shoot ratio in individual trees globally. *New Phytologist*, *217*(1), 8–11.

López-Mársico, L., Altesor, A., Oyarzabal, M., Baldassini, P., & Paruelo, J. M. (2015). Grazing increases below-ground biomass and net primary production in a temperate grassland. *Plant and Soil*, *392*(1), 155–162. https://doi.org/10.1007/s11104-015-2452-2

Luo, Z., Luo, Y., Wang, G., Xia, J., & Peng, C. (2020). Warming-induced global soil carbon loss attenuated by downward carbon movement. *Global Change Biology*, *00*, 1–13.

Luo, Z., Wang, G., & Wang, E. (2019). Global subsoil organic carbon turnover times dominantly controlled by soil properties rather than climate. *Nature Communications*, *10*(1), 3688.

Makkonen, K., & Helmisaari, H.-S. (1999). Assessing fine-root biomass and production in a scots pine stand–comparison of soil core and root ingrowth core methods. *Plant and Soil*, *210*(1), 43–50.

Malhi, Y., Girardin, C. A. J., Goldsmith, G. R., Doughty, C. E., Salinas, N., Metcalfe, D. B., Huasco, W. H., Silva-Espejo, J. E., Aguilla-Pasquell, J. D., Amézquita, F. F., Aragão, L. E. O. C., Guerrieri, R., Ishida, F. Y., Bahar, N. H. A., Farfan-Rios, W., Phillips, O. L., Meir, P., & Silman, M. (2017). The variation of productivity and its allocation along a tropical elevation gradient: A whole carbon budget perspective. *New Phytologist*, *214*(3), 1019–1032.

McCarthy, H. R., Oren, R., Johnsen, K. H., Gallet-Budynek, A., Pritchard, S. G., Cook, C. W., LaDeau, S. L., Jackson, R. B., & Finzi, A. C. (2010). Re-assessment of plant carbon dynamics at the Duke free-air CO_2 enrichment site: Interactions of atmospheric CO_2 with nitrogen and water availability over stand development. *New Phytologist*, *185*(2), 514–528.

McCormack, M. L., Dickie, I. A., Eissenstat, D. M., Fahey, T. J., Fernandez, C. W., Guo, D. L., Helmisaari, H.-S., Hobbie, E. A., Iversen, C. M., Jackson, R. B., Leppälammi-Kujansuu, J., Norby, R. J., Phillips, R. P., Pregitzer, K. S., Pritchard, S. G., Rewald, B., & Zadworny, M. (2015). Redefining fine roots improves understanding of below-ground contributions to terrestrial biosphere processes. *New Phytologist*, *207*(3), 505–518.

Meyer, H., & Pebesma, E. (2021). Predicting into unknown space? Estimating the area of applicability of spatial prediction models. *Methods in Ecology and Evolution*, *12*(9), 1620–1633. https://doi.org/10.1111/2041-210x.13650

Meyer, H., & Pebesma, E. (2022). Machine learning-based global maps of ecological variables and the challenge of assessing them. *Nature Communications*, *13*(1), 2208. https://doi.org/10.1038/s41467-022-29838-9

Meyer, H., Reudenbach, C., Hengl, T., Katurji, M., & Nauss, T. (2018). Improving performance of spatio-temporal machine learning models using forward feature selection and target-oriented validation. *Environmental Modelling & Software*, *101*, 1–9. https://doi.org/10.1016/j.envsoft.2017.12.001

Milchunas, D. G. (2009). Estimating root production: Comparison of 11 methods in shortgrass steppe and review of biases. *Ecosystems*, *12*(8), 1381–1402.

Milchunas, D. G., & Lauenroth, W. K. (2001). Belowground primary production by carbon isotope decay and long-term root biomass dynamics. *Ecosystems*, *4*(2), 139–150.

Mokany, K., Raison, R. J., & Prokushkin, A. S. (2006). Critical analysis of root: Shoot ratios in terrestrial biomes. *Global Change Biology*, *12*(1), 84–96.

Olson, D. M., Dinerstein, E., Wikramanayake, E. D., Burgess, N. D., Powell, G. V., Underwood, E. C., D'amico, J. A., Itoua, I., Strand, H. E., Morrison, J. C., Loucks, C. J., Allnutt, T. F., Ricketts, T. H., Kura, Y., Lamoreux, J. F., Wettengel, W. W., Hedao, P., & Kassem, K. R. (2001). Terrestrial ecoregions of the world: A new map of life on earth: A new global map of terrestrial ecoregions provides an innovative tool for conserving biodiversity. *Bioscience*, *51*(11), 933–938.

R Development Core Team. (2021). *R: A language and environment for statistical computing*. R Foundation for Statistical Computing. http://www.R-project.org

Raich, J. W., & Nadelhoffer, K. J. (1989). Belowground carbon allocation in forest ecosystems: Global trends. *Ecology*, *70*(5), 1346–1354.

Reich, P. B., Sendall, K. M., Stefanski, A., Rich, R. L., Hobbie, S. E., & Montgomery, R. A. (2018). Effects of climate warming on photosynthesis in boreal tree species depend on soil moisture. *Nature*, *562*(7726), 263–267. https://doi.org/10.1038/s41586-018-0582-4

Sun, Y., Yang, Y., Zhao, X., Tang, Z., Wang, S., & Fang, J. (2021). Global patterns and climatic drivers of above-and belowground net primary productivity in grasslands. *Science China Life Sciences*, *64*, 739–751.

Vicca, S., Stocker, B. D., Reed, S., Wieder, W. R., Bahn, M., Fay, P. A., Janssens, I. A., Lambers, H., Peñuelas, J., Piao, S., Rebel, K. T., Sardans, J., Sigurdsson, B. D., Van Sundert, K., Wang, Y.-P., Zaehle, S., & Ciais, P. (2018). Using research networks to create the comprehensive datasets needed to assess nutrient availability as a key determinant of terrestrial carbon cycling. *Environmental Research Letters*, *13*(12), 125006. https://doi.org/10.1088/1748-9326/aaeae7

Walker, M. D., Wahren, C. H., Hollister, R. D., Henry, G. H. R., Ahlquist, L. E., Alatalo, J. M., Bret-Harte, M. S., Calef, M. P., Callaghan, T. V., Carroll, A. B., Epstein, H. E., Jonsdottir, I. S., Klein, J. A., Magnusson, B., Molau, U., Oberbauer, S. F., Rewa, S. P., Robinson, C. H., Shaver, G. R., … Wookey, P. A. (2006). Plant community responses to experimental warming across the tundra biome. *Proceedings of the National Academy of Sciences of the United States of America*, *103*(5), 1342–1346. https://doi.org/10.1073/pnas.0503198103

Wang, D., Heckathorn, S. A., Wang, X., & Philpott, S. M. (2012). A meta-analysis of plant physiological and growth responses to temperature and elevated CO 2. *Oecologia*, *169*(1), 1–13.

Way, D. A., & Oren, R. (2010). Differential responses to changes in growth temperature between trees from different functional groups and biomes: A review and synthesis of data. *Tree Physiology*, *30*(6), 669–688. https://doi.org/10.1093/treephys/tpq015

Wieder, W. R., Cleveland, C. C., Smith, W. K., & Todd-Brown, K. (2015). Future productivity and carbon storage limited by terrestrial nutrient availability. *Nature Geoscience*, *8*(6), 441–444.

Xu, X., Luo, Y., Shi, Z., Zhou, X., & Li, D. (2014). Consistent proportional increments in responses of belowground net primary productivity to long-term warming and clipping at various soil depths in a tallgrass prairie. *Oecologia*, *174*(3), 1045–1054. https://doi.org/10.1007/s00442-013-2828-z

Yuan, Z., & Chen, H. Y. (2010). Fine root biomass, production, turnover rates, and nutrient contents in boreal forest ecosystems in relation to species, climate, fertility, and stand age: Literature review and meta-analyses. *Critical Reviews in Plant Sciences*, *29*(4), 204–221.

Zhang, X. Y., & Wang, W. (2015). The decomposition of fine and coarse roots: Their global patterns and controlling factors. *Scientific Reports*, *5*, 10.

Zhao, M. S., & Running, S. W. (2010). Drought-induced reduction in global terrestrial net primary production from 2000 through 2009. *Science*, *329*(5994), 940–943.

Zuur, A. F., Ieno, E. N., & Elphick, C. S. (2010). A protocol for data exploration to avoid common statistical problems. *Methods in Ecology and Evolution*, *1*(1), 3–14.

SUPPORTING INFORMATION

Additional supporting information can be found online in the Supporting Information section at the end of this article.

How to cite this article: Xiao, L., Wang, G., Chang, J., Chen, Y., Guo, X., Mao, X., Wang, M., Zhang, S., Shi, Z., Luo, Y., Cheng, L., Yu, K., Mo, F., & Luo, Z. (2023). Global depth distribution of belowground net primary productivity and its drivers. *Global Ecology and Biogeography*, *32*, 1435–1451. https://doi.org/10.1111/geb.13705

APPENDIX A

Data sources

An, J. Y., Park, B. B., Chun, J. H., & Osawa, A. (2017). Litterfall production and fine root dynamics in cool-temperate forests. *PloS ONE*, 2(6), e0180126.

Aragão, L. E. O. C., Malhi, Y., Metcalfe, D. B., Silva-Espejo, J. E., Jiménez, E., Navarrete, D., Almeida, S., Costa, A. C. L., Salinas, N., Phillips, O. L., Anderson, L. O., Alvarez, E., Baker, T. R., Goncalvez, P. H., Huamán-Ovalle, J., Mamani-Solórzano, M., Meir, P., Monteagudo, A., Patiño, S., … Vásquez, R. (2009). Above-and below-ground net primary productivity across ten Amazonian forests on contrasting soils. *Biogeosciences*, (12), 2759–2778.

Basuki, I., Kauffman, J. B., Peterson, J., Anshari, G., & Murdiyarso, D. (2019). Land cover changes reduce net primary production in tropical coastal peatlands of West Kalimantan, Indonesia. *Mitigation and Adaptation Strategies for Global Change*, 4(4), 557–573.

Bond-Lamberty, B., Wang, C., & Gower, S. T. (2004). Net primary production and net ecosystem production of a boreal black spruce wildfire chronosequence. *Global Change Biology*, 10(4), 473–487.

Campioli, M., Michelsen, A., Demey, A., Vermeulen, A., Samson, R., & Lemeur, R. (2009). Net primary production and carbon stocks for subarctic mesic–dry tundras with contrasting microtopography, altitude, and dominant species. *Ecosystems*, 2(5), 760–776.

Dai, L., Ke, X., Du, Y., Zhang, F., Li, Y., Li, Q., Lin, L., Peng, C., Shu, K., Cao, G., & Guo, X. (2019). Nitrogen controls the net primary production of an alpine Kobresia meadow in the northern Qinghai-Tibet Plateau. *Ecology and Evolution*, (15), 8865–8875.

Doughty, C. E., Metcalfe, D. B., da Costa, M. C., de Oliveira, A. A., Neto, G. F. C., Silva, J. A., Aragao, L. E. O. C., Almeida, S. S., Quesada, C. A., Girardin, C. A. J., Halladay, K., da Costa, A. C. L., & Malhi, Y. (2014). The production, allocation and cycling of carbon in a forest on fertile terra preta soil in eastern Amazonia compared with a forest on adjacent infertile soil. *Plant Ecology & Diversity*, (1-2), 41-53.

Fisk, M. C., Schmidt, S. K., & Seastedt, T. R. (1998). Topographic patterns of above-and belowground production and nitrogen cycling in alpine tundra. *Ecology*, 9(7), 2253–2266.

Frank, D. A. (2007). Drought effects on above-and belowground production of a grazed temperate grassland ecosystem. *Oecologia*, 52(1), 131–139.

Gao, Y. Z., Chen, Q., Lin, S., Giese, M., & Brueck, H. (2011). Resource manipulation effects on net primary production, biomass allocation and rain-use efficiency of two semiarid grassland sites in Inner Mongolia, China. *Oecologia*, 65(4), 855–864.

Gilmanov, T. G., & Oechel, W. C. (1995). New estimates of organic matter reserves and net primary productivity of the North American tundra ecosystems. *Journal of Biogeography*, 23–741.

Girardin, C. A. J., Malhi, Y., Aragao, L. E. O. C., Mamani, M., Huaraca Huasco, W., Durand, L., Feeley, K. J., Rapp, J., Silva-Espejo, J. E., Silman, M., Salinas, N., & Whittaker, R. J. (2010). Net primary productivity allocation and cycling of carbon along a tropical forest elevational transect in the Peruvian Andes. *Global Change Biology*, 6(12), 3176–3192.

Girardin, C. A., Espejob, J. E. S., Doughty, C. E., Huasco, W. H., Metcalfe, D. B., Durand-Baca, L., Marthews, T. R., Aragao, Luiz E. O. C., Farfan-Rios, W., Garcia-Cabrera, K., Halladay, K., Fisher, J. B., Galiano-Cabrera, D. F., Huaraca-Quispe, L. P., Alzamora-Taype, I., Eguiluz-Mora, L., Salinas-Revilla, N., Silman, M. R., Meir, P., & Malhi, Y. (2014). Productivity and carbon allocation in a tropical montane cloud forest in the Peruvian Andes. *Plant Ecology & Diversity*, (1-2), 107–123.

Gower, S. T., Krankina, O., Olson, R. J., Apps, M., Linder, S., & Wang, C. (2001). Net primary production and carbon allocation patterns of boreal forest ecosystems. *Ecological Applications*, 1(5), 1395–1411.

Gower, S. T., Vogel, J. G., Norman, J. M., Kucharik, C. J., Steele, S. J., & Stow, T. K. (1997). Carbon distribution and aboveground net primary production in aspen, jack pine, and black spruce stands in Saskatchewan and Manitoba, Canada. *Journal of Geophysical Research: Atmospheres*, 02(D24), 29029–29041.

Helmisaari, H. S., Makkonen, K., Kellomäki, S., Valtonen, E., & Mälkönen, E. (2002). Below-and above-ground biomass, production and nitrogen use in Scots pine stands in eastern Finland. *Forest Ecology and Management*, 65(1-3), 317–326.

Herbert, D. A., & Fownes, J. H. (1999). Forest productivity and efficiency of resource use across a chronosequence of tropical montane soils. *Ecosystems*, (3), 242–254.

Hertel, D., Moser, G., Culmsee, H., Erasmi, S., Horna, V., Schuldt, B., & Leuschner, C. (2009). Below-and above-ground biomass and net primary production in a paleotropical natural forest (Sulawesi, Indonesia) as compared to neotropical forests. *Forest Ecology and Management*, 58(9), 1904–1912.

Huasco, W. H., Girardin, C. A., Doughty, C. E., Metcalfe, D. B., Baca, L. D., Silva-Espejo, J. E., Cabrera, D. G., Aragão, L. E. O. C., Davila, A. R., Marthews,T. R., Huaraca-Quispe, L. P., Alzamora-Taype, I., Mora, L. E., Farfán-Rios, W., Cabrera, K. G., Halladay, K., Salinas-Revilla, N., Silman, M. R., Meir, P., & Malhi, Y. (2014). Seasonal production, allocation and cycling of carbon in two mid-elevation tropical montane forest plots in the Peruvian Andes. *Plant Ecology & Diversity*, (1-2), 125–142.

Hui, D., & Jackson, R.B. (2006). Geographical and interannual variability in biomass partitioning in grassland ecosystems: A synthesis of field data. *New Phytologist*, 69(1), 85–93.

Kalyn, A. L., & Van Rees, K. C. J. (2006). Contribution of fine roots to ecosystem biomass and net primary production in black spruce, aspen, and jack pine forests in Saskatchewan. *Agricultural and Forest Meteorology*, 40(1–4), 236–243.

Li, J., Lin, S., Taube, F., Pan, Q., & Dittert, K. (2011). Above and belowground net primary productivity of grassland influenced by supplemental water and nitrogen in Inner Mongolia. *Plant and Soil*, 40(1-2), 253–264.

Liu, H., Mi, Z., Lin, L., Wang, Y., Zhang, Z., Zhang, F., Wang, H., Liu, L., Zhu, B., Cao, G., Zhao, X., Sanders, N. J., Classen, A., Reich, P. B., & He, J.S. (2018). Shifting plant species composition in response to climate change stabilizes grassland primary production. *Proceedings of the National Academy of Sciences of the United States of America*, 15(16), 4051–4056.

Maeda, Y., Tashiro, N., Enoki, T., Urakawa, R., & Hishi, T. (2018). Effects of species replacement on the relationship between net primary production and soil nitrogen availability along a topographical gradient: Comparison of belowground allocation and nitrogen use efficiency between natural forests and plantations. *Forest Ecology and Management*, *22*, 214-222.

Malhi, Y., Aragao, L. E. O., Metcalfe, D. B., Paiva, R., Quesada, C. A., Almeida, S., Anderson, L., Brando, P., Chambers, J. Q., Da Costa, A. C. L., Hutyra, L. R., Oliveira, P., Patiño, S., Pyle, E. H., Robertson, A. L., & Teixeira, L. M. (2009). Comprehensive assessment of carbon productivity, allocation and storage in three Amazonian forests. *Global Change Biology*, 5(5), 1255–1274.

Malhi, Y., Doughty, C. E., Goldsmith, G. R., Metcalfe, D. B., Girardin, C. A., Marthews, T. R., del Aguila-Pasquel, J., Aragão, L. E. O. C., Araujo-Murakami, A., Brando, P., da Costa, A. C. L., Silva-Espejo, J. E., Amézquita, F. F., Galbraith, D. R., Quesada, C. A., Rocha, W., Salinas-Revilla, N., Silvério, D., Meir, P., Phillips, O. L. (2015). The linkages between photosynthesis, productivity, growth and biomass in lowland Amazonian forests. *Global Change Biology*, 1(6), 2283–2295.

Malhi, Y., Farfán Amézquita, F., Doughty, C. E., Silva-Espejo, J. E., Girardin, C. A., Metcalfe, D. B., Aragão, L. E. O. C., Huaraca-Quispe, L. P., Alzamora-Taype, I., Eguiluz-Mora, L., Marthews, T. R., Halladay, K., Quesada, C. A., Robertson, A. L., Fisher, J. B., Zaragoza-Castells, J., Rojas-Villagra, C. M., Pelaez-Tapia, Y., Salinas, N., … Phillips, O. L. (2014). The productivity, metabolism and carbon cycle of two lowland tropical forest plots in south-western Amazonia, Peru. *Plant Ecology & Diversity*, (1-2), 85–105.

Malhi, Y., Girardin, C. A., Goldsmith, G. R., Doughty, C. E., Salinas, N., Metcalfe, D. B., Huasco, W. H., Silva-Espejo, J. E., Del Aguilla-Pasquell, J., Amézquita, F. F., Aragão, L. E. O. C., Guerrieri, R., Ishida, F. Y., Bahar, N. H. A., Farfan-Rios, W., Phillips, O. L., Meir, P., & Silman, M. (2017). The variation of productivity and its allocation along a tropical elevation gradient: A whole carbon budget perspective. *New Phytologist*, 14(3), 1019–1032.

Martinez, C., Alberti, G., Cotrufo, M. F., Magnani, F., Zanotelli, D., Camin, F., Gianelle, D., Cescatti, A., & Rodeghiero, M. (2016). Belowground carbon allocation patterns as determined by the in-growth soil core 13C technique across different ecosystem types. *Geoderma*, 63, 140–150.

Martinez-Yrizar, A., Maass, J. M., Pérez-Jiménez, L. A., & Sarukhán, J. (1996). Net primary productivity of a tropical deciduous forest ecosystem in western Mexico. *Journal of Tropical Ecology*, 2(1), 169–175.

Moore, S., Adu-Bredu, S., Duah-Gyamfi, A., Addo-Danso, S. D., Ibrahim, F., Mbou, A. T., de Grandcourt, A., Valentini, R., Nicolini, G., Djagbletey, G., Owusu-Afriyie, K., Gvozdevaite, A., Oliveras, I., Ruiz-Jaen, M. C., & Malhi, Y. (2018). Forest biomass, productivity and carbon cycling along a rainfall gradient in West Africa. *Global Change Biology*, 4(2), e496–e510.

Moser, G., Leuschner, C., Hertel, D., Graefe, S., Soethe, N., & Iost, S. (2011). Elevation effects on the carbon budget of tropical mountain forests (S Ecuador): The role of the belowground compartment. *Global Change Biology*, 7(6), 2211–2226.

Newman, G. S., Arthur, M. A., & Muller, R. N. (2006). Above-and belowground net primary production in a temperate mixed deciduous forest. *Ecosystems*, (3), 317–329.

Ni, J. (2004). Estimating net primary productivity of grasslands from field biomass measurements in temperate northern China. *Plant Ecology*, 74(2), 217–234.

Niu, B., Zeng, C., Zhang, X., He, Y., Shi, P., Tian, Y., Feng, Y., Li, M., Wang, Z., Wang, X., & Cao, Y. (2019). High below-ground productivity allocation of alpine grasslands on the Northern Tibet. *Plants*, (12), 535.

Oliver, V., Cochrane, N., Magnusson, J., Brachi, E., Monaco, S., Volante, A., Courtois, B., Vale, G., Price, A., & Teh, Y. A. (2019). Effects of water management and cultivar on carbon dynamics, plant productivity and biomass allocation in European rice systems. *Science of The Total Environment*, *85*, 1139–1151.

Ram, J., Singh, J. S., & Singh, S. P. (1989). Plant biomass, species diversity and net primary production in a central Himalayan high altitude grassland. *The Journal of Ecology*, *77*, 456–468.

Riutta, T., Malhi, Y., Kho, L. K., Marthews, T. R., Huaraca Huasco, W., Khoo, M., Tan, S., Turner, E., Reynolds, G., Both, S., Burslem, D. F. R. P., Arn Teh, Y., Vairappan, C. S., Majalap, N., & Ewers, R. M. (2018). Logging disturbance shifts net primary productivity and its allocation in Bornean tropical forests. *Global Change Biology*, 4(4), 2913–2928.

Ruess, R. W., Cleve, K. V., Yarie, J., & Viereck, L. A. (1996). Contributions of fine root production and turnover to the carbon and nitrogen cycling in taiga forests of the Alaskan interior. *Canadian Journal of Forest Research*, 6(8), 1326–1336.

Ryan, M. G., Lavigne, M. B., & Gower, S. T. (1997). Annual carbon cost of autotrophic respiration in boreal forest ecosystems in relation to species and climate. *Journal of Geophysical Research: Atmospheres*, 02(D24), 28871–28883.

Sierra, C. A., Harmon, M. E., Moreno, F. H., Orrego, S. A., & Del Valle, J. I. (2007). Spatial and temporal variability of net ecosystem production in a tropical forest: Testing the hypothesis of a significant carbon sink. *Global Change Biology*, 3(4), 838–853.

Steele, S. J., Gower, S. T., Vogel, J. G., & Norman, J. M. (1997). Root mass, net primary production and turnover in aspen, jack pine and black spruce forests in Saskatchewan and Manitoba, Canada. *Tree physiology*, 7(8-9), 577–587.

Tan, Z., Zhang, Y., Yu, G., Sha, L., Tang, J., Deng, X., & Song, Q. (2010). Carbon balance of a primary tropical seasonal rain forest. *Journal of Geophysical Research: Atmospheres*, *115*(D00H26), 10.1029/2009JD012913

Tateno, R., Hishi, T., & Takeda, H. (2004). Above-and belowground biomass and net primary production in a cool-temperate deciduous forest in relation to topographical changes in soil nitrogen. *Forest Ecology and Management*, 93(3), 297–306.

Van Do, T., Sato, T., Saito, S., & Kozan, O. (2015). Fine-root production and litterfall: Main contributions to net primary production in an old-growth evergreen broad-leaved forest in southwestern Japan. *Ecological Research*, 30(5), 921–930.

Vogt, K. A., Vogt, D. J., Palmiotto, P. A., Boon, P., O'Hara, J., & Asbjornsen, H. (1996). Review of root dynamics in forest ecosystems grouped by climate, climatic forest type and species. *Plant and Soil*, 87(2), 159–219.

Wang, C., Gower, S. T., Wang, Y., Zhao, H., Yan, P., & Bond-Lamberty, B. P. (2001). The influence of fire on carbon distribution and net primary production of boreal *Larix gmelinii* forests in north-eastern China. *Global Change Biology*, (6), 719–730.

Wang, J., Gao, Y., Zhang, Y., Yang, J., Smith, M. D., Knapp, A. K., Eissenstat, D. M., & Han, X. (2019). Asymmetry in above- and belowground productivity responses to N addition in a semi-arid temperate steppe. *Global Change Biology*, *5*(9), 2958–2969.

Xiao, C. W., Yuste, J. C., Janssens, I. A., Roskams, P., Nachtergale, L., Carrara, A., Sanchez, B. Y., & Ceulemans, R. (2003). Above-and belowground biomass and net primary production in a 73-year-old Scots pine forest. *Tree Physiology*, 3(8), 505–516.

Xu, X., Niu, S., Sherry, R. A., Zhou, X., Zhou, J., & Luo, Y. (2012). Interannual variability in responses of belowground net primary productivity (NPP) and NPP partitioning to long-term warming and clipping in a tallgrass prairie. *Global Change Biology*, 8(5), 1648–1656.

Yang, Y. S., Chen, G. S., Guo, J. F., Xie, J. S., & Wang, X. G. (2007). Soil respiration and carbon balance in a subtropical native forest and two managed plantations. *Plant Ecology*, 93(1), 71–84.

Yuste, J. C., Konôpka, B., Janssens, I. A., Coenen, K., Xiao, C. W., & Ceulemans, R. (2005). Contrasting net primary productivity and carbon distribution between neighbouring stands of *Quercus robur* and *Pinus sylvestris*. *Tree Physiology*, 5(6), 701–712.

Zhang, B., Cadotte, M. W., Chen, S., Tan, X., You, C., Ren, T., Chen, M., Wang, S., Li, W., Chu, C., Jiang, L., Bai, Y., Huang, J., & Han, X. (2019). Plants alter their vertical root distribution rather than biomass allocation in response to changing precipitation. *Ecology*, 100(11), e02828.

Zhang, F., Quan, Q., Song, B., Sun, J., Chen, Y., Zhou, Q., & Niu, S. (2017). Net primary productivity and its partitioning in response to precipitation gradient in an alpine meadow. *Scientific Reports*, (1), 15193.